**Title: Artificial intelligence to detect malignant eyelid tumors from photographic images**

**Supplementary Information**

1. **Supplementary Figure 1 Confusion matrices of four deep learning algorithms in the internal and external test sets.** a, Internal test set. b, External test set. BET, benign eyelid tumor. MET, malignant eyelid tumor.

2. **Supplementary Figure 2. Visualization by t-SNE for presenting the separability of the features learned by four different deep learning algorithms.** a, Internal test set. b, External test set. t-SNE, t-distributed stochastic neighbor embedding. BET, benign eyelid tumor. MET, malignant eyelid tumor.

3. **Supplementary Figure 3. Performance of the deep learning system in images of eyelid tumors of uncertain malignant nature.** ETUMA, eyelid tumors of uncertain malignant nature.

4. **Supplementary Figure 4. False-negative and false-positive findings by the deep learning system in the internal and external test sets.** BCC, basal cell carcinomas. SCC, squamous cell carcinomas. SCP, squamous cell papilloma.

5. **Supplementary Figure 5. Examples of incorrectly classified images by the deep learning system.** a, Images of malignant eyelid tumors (MET) were misclassified by the system as benign eyelid tumors (BET). b, Images of BET were misclassified by the system as MET.

6. **Supplementary Figure 6. Confusion matrices of three ophthalmologists in the external test set.** BET, benign eyelid tumor. MET, malignant eyelid tumor.

7. **Supplementary Figure 7. Diagram showing an overview of the proposed eyelid tumor detection system.** Convolution layers are employed to filter an input image and extract effective features. Feature maps show the output of previous layers. Region proposals indicate a network that outputs interesting regions (eyelid tumors) from feature maps. ROI pooling is a layer that conducts maximum pooling in region proposals of non-uniform sizes for obtaining fixed-size feature maps. RCNN, region-based convolutional neural network. ROI, region of interest.

8. **Supplementary Figure 8. Flow diagram of the development and assessment of the deep learning classification system.**

9. **Supplementary Table 1 Performance of the deep learning system vs. ophthalmologists in the external test set.**

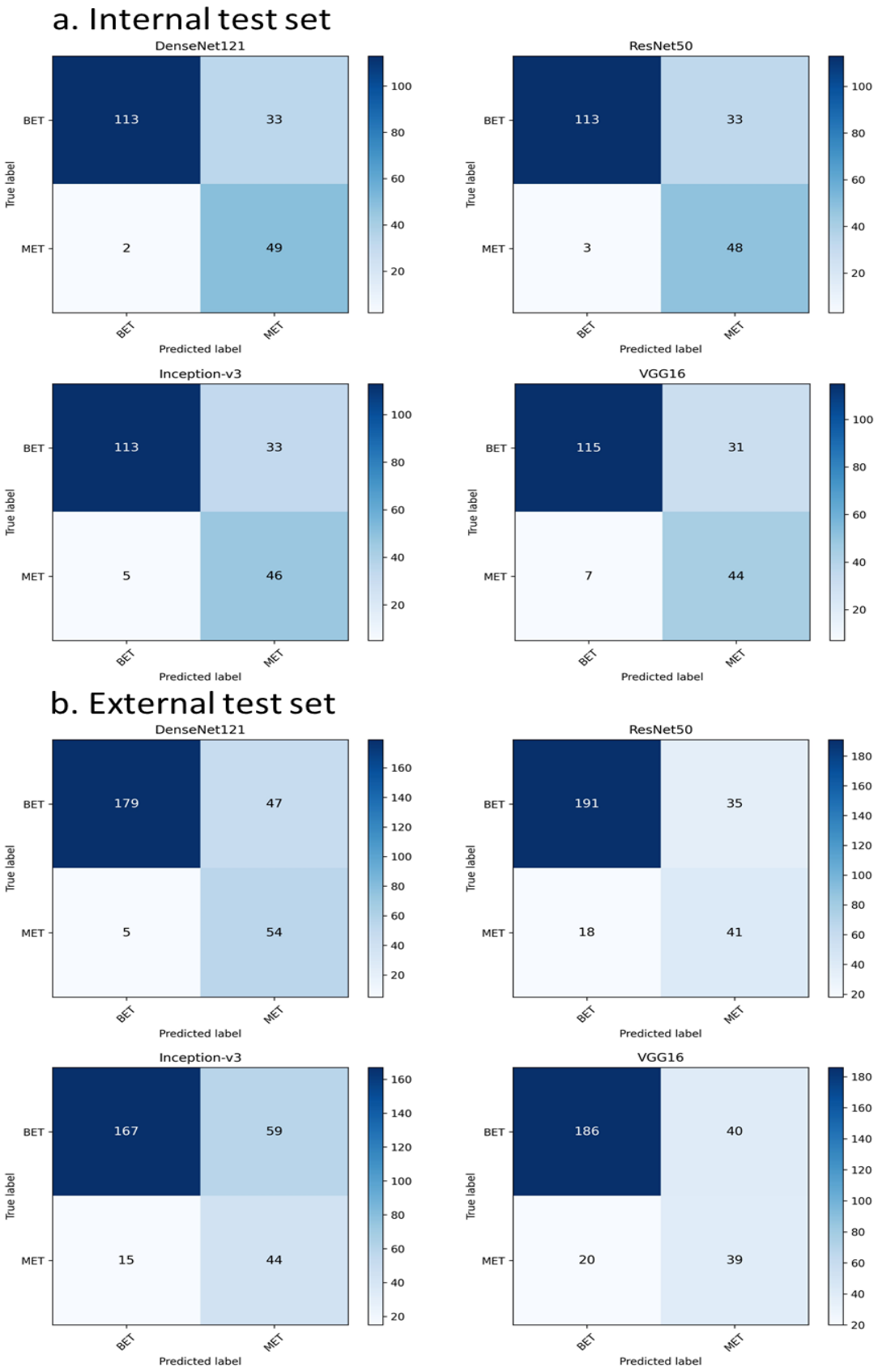


**Supplementary Figure 1. Confusion matrices of four deep learning algorithms in the internal and external test sets.** a, Internal test set. b, External test set. BET, benign eyelid tumor. MET, malignant eyelid tumor.


**Supplementary Figure 2. Visualization by t-SNE for presenting the separability of the features learned by four different deep learning algorithms.** a, Internal test set. b, External test set. t-SNE, t-distributed stochastic neighbor embedding. BET, benign eyelid tumor. MET, malignant eyelid tumor.

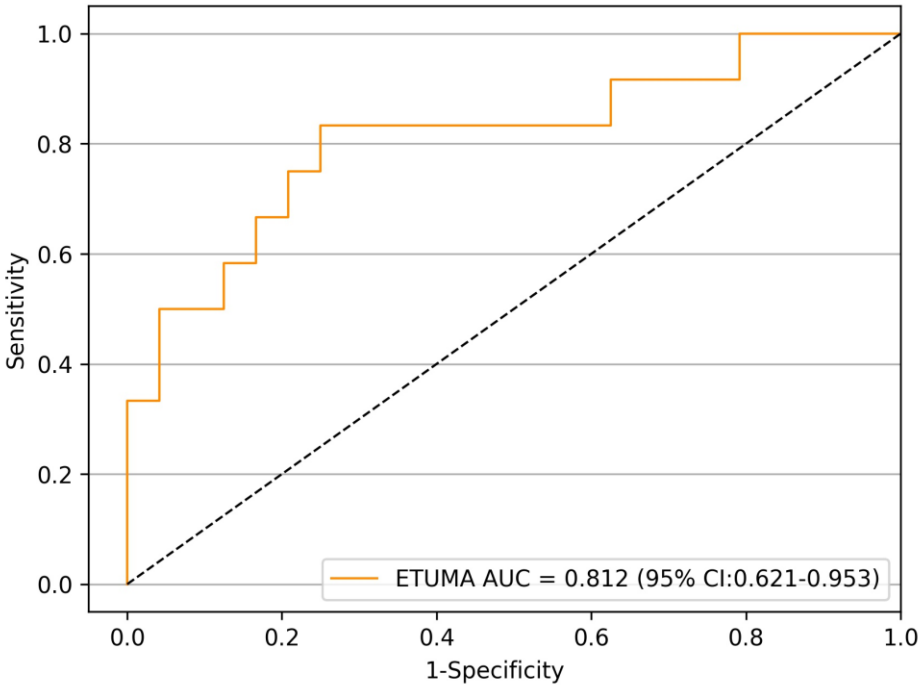


**Supplementary Figure 3. Performance of the deep learning system in images of eyelid tumors of uncertain malignant nature.** ETUMA, eyelid tumors of uncertain malignant nature.

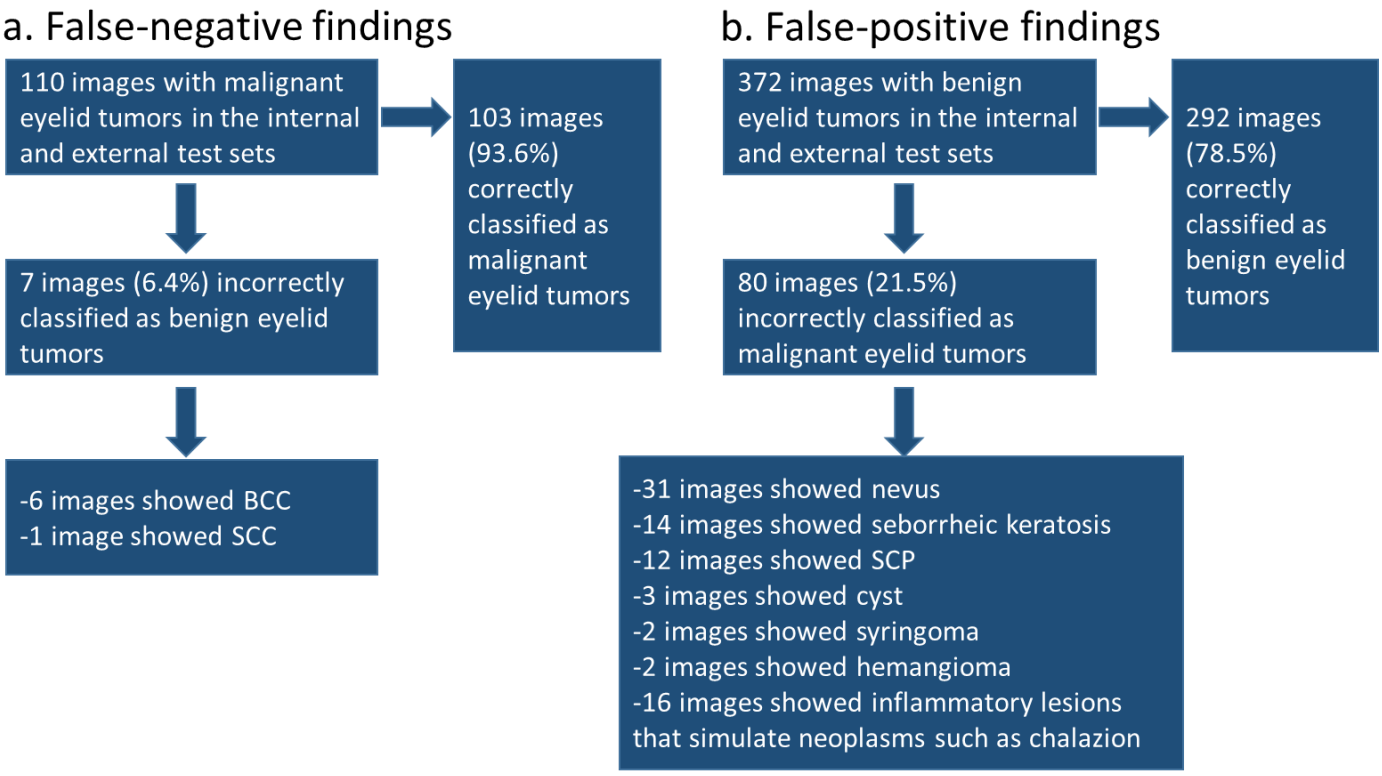


**Supplementary Figure 4. False-negative and false-positive findings by the deep learning system in the internal and external test sets.** BCC, basal cell carcinomas. SCC, squamous cell carcinomas. SCP, squamous cell papilloma.

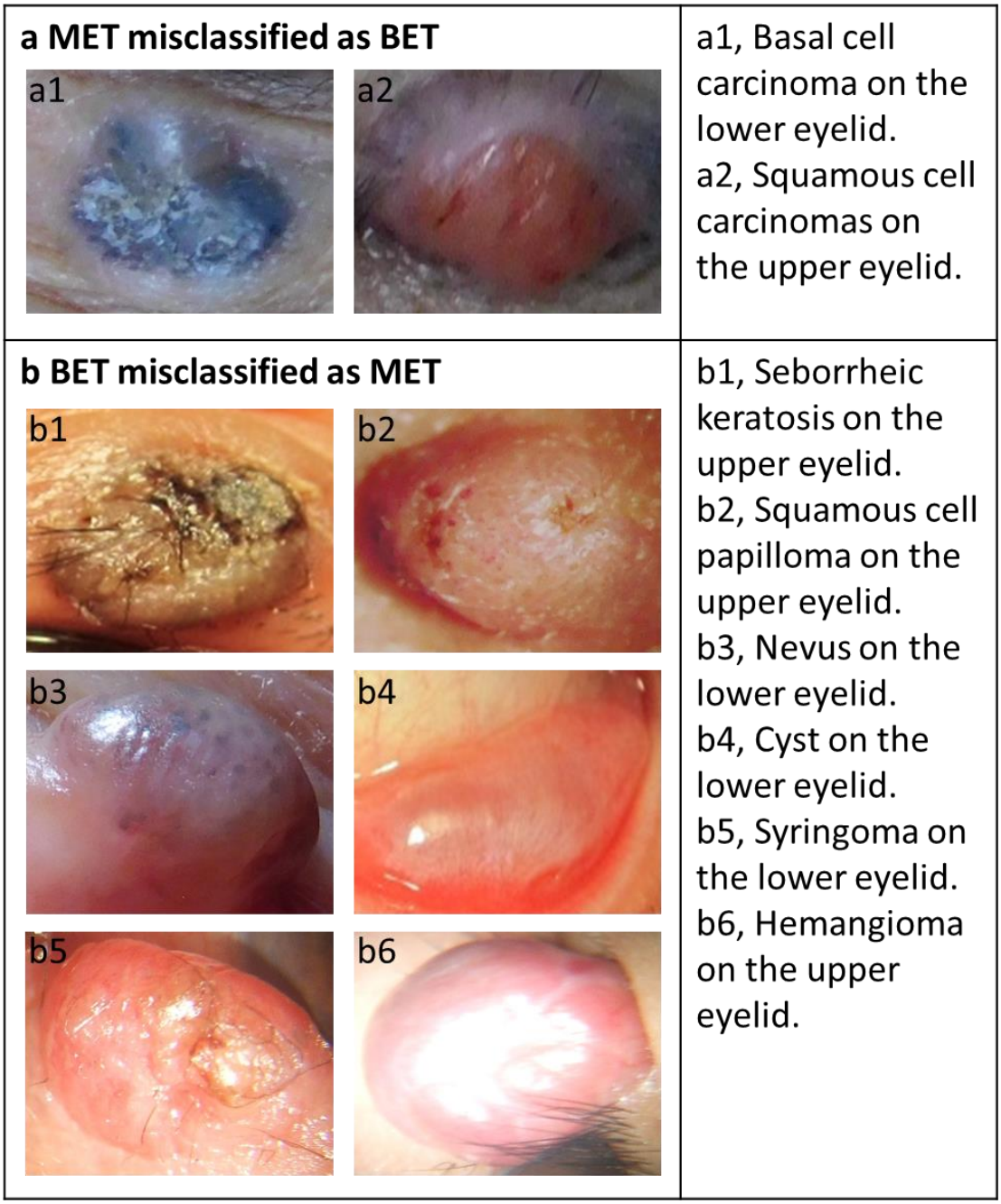


**Supplementary Figure 5. Examples of incorrectly classified images by the deep learning system.** a, Images of malignant eyelid tumors (MET) were misclassified by the system as benign eyelid tumors (BET). b, Images of BET were misclassified by the system as MET.

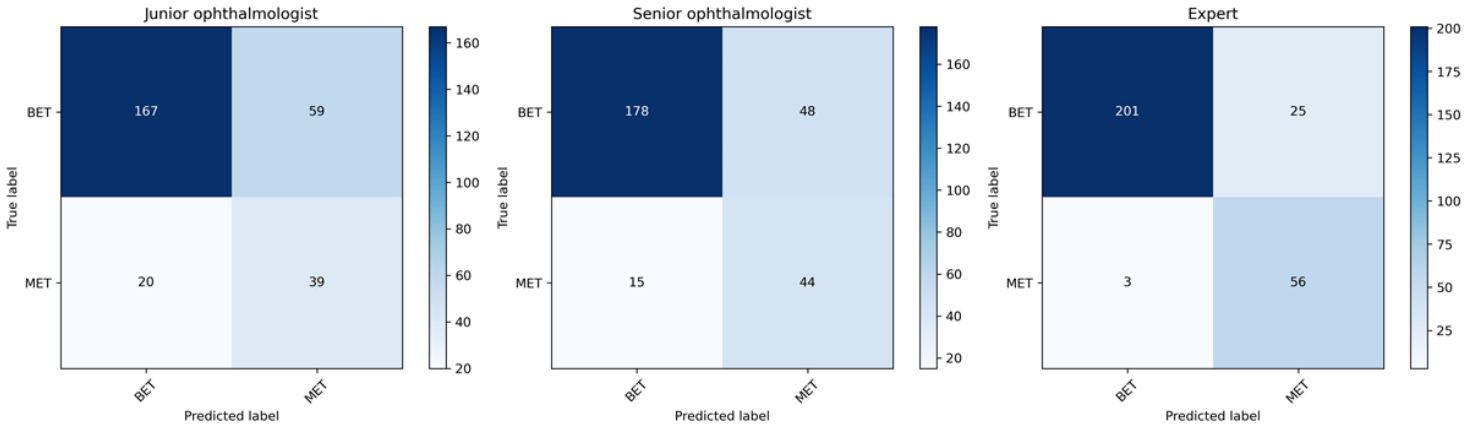


**Supplementary Figure 6. Confusion matrices of three ophthalmologists in the external test set.** BET, benign eyelid tumor. MET, malignant eyelid tumor.

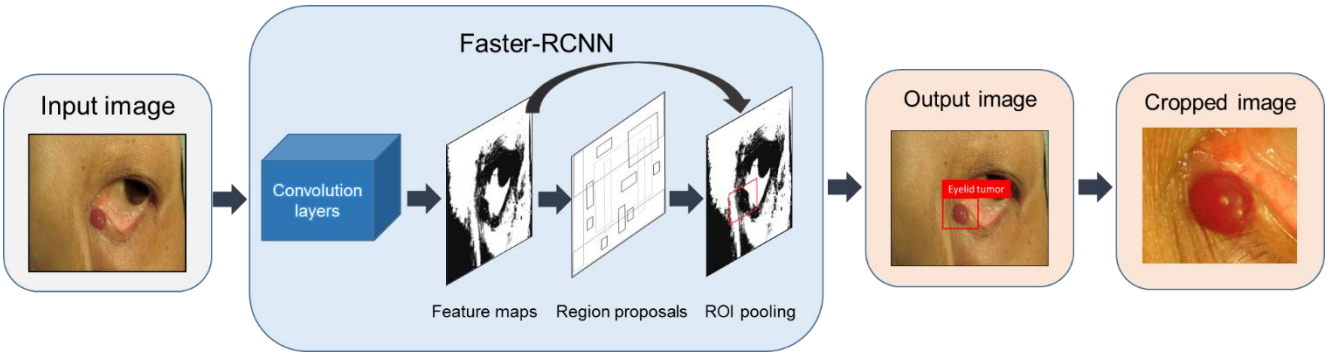


**Supplementary Figure 7. Diagram showing an overview of the proposed eyelid tumor detection system.** Convolution layers are employed to filter an input image and extract effective features. Feature maps show the output of previous layers. Region proposals indicate a network that outputs interesting regions (eyelid tumors) from feature maps. ROI pooling is a layer that conducts maximum pooling in region proposals of non-uniform sizes for obtaining fixed-size feature maps. RCNN, region-based convolutional neural network. ROI, region of interest.

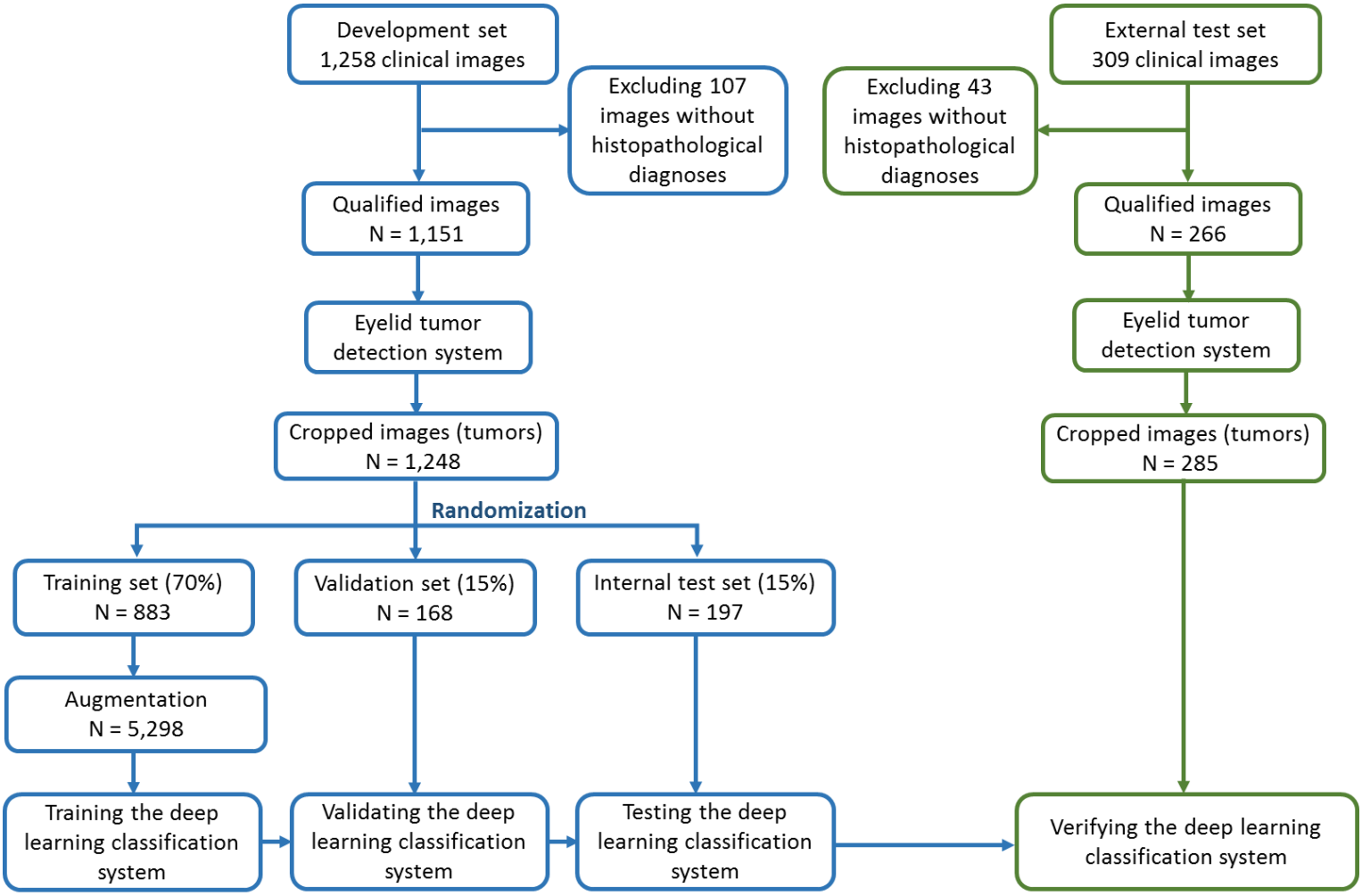


**Supplementary Figure 8. Flow diagram of the development and assessment of the deep learning classification system.**

**Supplementary Table 1 Performance of the deep learning system vs. ophthalmologists in the external test set.**

| | Deep learning system | Junior | Senior | Expert | *P1* | *P2* | *P3* |
|---|---|---|---|---|---|---|---|
| Sensitivity (95% CI) | 91.5% (84.4-98.6) | 66.1% (54.0-78.2) | 74.6% (63.5-85.7) | 94.9% (89.3-100) | < 0.001 | 0.006 | 0.688 |
| Specificity (95% CI) | 79.2% (73.9-84.5) | 73.9% (68.2-79.6) | 78.8% (73.4-84.1) | 88.9% (84.8-93.0) | 0.195 | 1.000 | 0.004 |
| Accuracy (95% CI) | 81.8% (77.3-86.2) | 72.3% (67.1-77.5) | 77.9% (73.1-82.7) | 90.2% (86.7-93.6) | 0.006 | 0.228 | 0.003 |

"Junior" indicates an ophthalmologist with 3 years of clinical experience. "Senior" indicates an ophthalmologist with 7 years of clinical experience. "Expert" indicates an ophthalmologist with 15 years of clinical experience. *P1* denotes the p-value that was calculated between the system and junior ophthalmologist using the two-sided McNemar test. *P2* denotes the p-value that was calculated between the system and senior ophthalmologist using the two-sided McNemar test. *P3* denotes the p-value that was calculated between the system and the expert using the two-sided McNemar test. CI, confidence interval.